Spin-density-wave state in $(TMTSF)_2PF_6$: A ^{77}Se NMR study at high magnetic fields

S. Valfells
Department of Physics, Boston University, Boston, Massachusetts 02215

P. Kuhns and A. Kleinhammes
National High Magnetic Field Laboratory, 1800 East Paul Dirac Drive, Tallahassee, Florida 32310

J. S. Brooks
Department of Physics, Boston University, Boston, Massachusetts 02215;
National High Magnetic Field Laboratory, 1800 East Paul Dirac Drive, Tallahassee, Florida 32310;
and Department of Physics, Florida State University, Tallahassee, Florida 32306-4005

W. Moulton
National High Magnetic Field Laboratory, 1800 East Paul Dirac Drive, Tallahassee, Florida 32310
and Department of Physics, Florida State University, Tallahassee, Florida 32306-4005

S. Takasaki, J. Yamada, and H. Anzai
Himeji Institute of Technology, 2167 Shosya, Himeji, Hyogo 671-22, Japan
(Received 14 November 1996; revised manuscript received 22 January 1997)

We present a nuclear magnetic resonance study of the low-temperature spin-density-wave (SDW) ground state in the quasi-one-dimensional conductor $(TMTSF)_2PF_6$ [bis-(tetramethyl-tetraselenafulvalene)hexafluorophosphate]. Using magnetic fields up to 22 T, we have measured the ^{77}Se spin-lattice (T_1^{-1}) and spin-spin relaxation rates (T_2^{-1}) above and below the SDW transition ($T_{SDW} \approx 12$ K). Between T_{SDW} and ≈ 4 K, we observe anomalously fast and Korringa-like T_1^{-1}; below 4 K, T_1^{-1} decays rapidly. A reduction in T_2^{-1} is also observed at 4 K, but the absorption linewidth does not change to within experimental error. We attribute this behavior to an incomplete SDW transition at T_{SDW}, leaving residual carriers at the Fermi level, and a subsequent consummation of the transition at 4 K. Our data below 4 K are consistent with a simple model of the temperature dependence of T_1^{-1} in a fully gapped and low-dimensional conductor. [S0163-1829(97)00929-6]

I. INTRODUCTION

The SDW state in $(TMTSF)_2PF_6$ [bis-(tetramethyl-tetraselenafulvalene)hexafluorophosphate] has been the subject of considerable experimental attention for more than a decade. Nevertheless, the detailed nature of its electronic structure is far from clear. While few doubt the existence of a nearly commensurate SDW with a BCS-like gap immediately below the 12 K transition temperature (reported values of T_{SDW} range from 11.1 to 12.1 K, the variation, presumably, caused by the impurity content of the samples[1]), the order of the phase change, the nature of the excitations of the SDW, and the existence of further phase changes at lower temperatures, approximately 3.5 and 1.5 K, are still controversial.

The motivation for the present study is the desire to better understand the metal-insulator, metal-superconductor transitions in low-dimensional conductors which give rise to broken symmetry density wave and superconducting ground states (for an overview, see Ref. 2). The nature of these transitions—which are driven by repulsive and attractive electron correlations—is particularly sensitive to the physical and electronic structure of these materials, and the ground states may be probed and/or altered by high magnetic fields. For example, the Bechgaard salts, of which $(TMTSF)_2PF_6$ and $(TMTSF)_2ClO_4$ are members, exhibit unusual properties in high magnetic fields, including field-induced spin density wave transitions (FISDW), anomalous quantum limit states, and anomalous quantum oscillation (and oscillation attenuation) behavior.[3,4]

NMR is a powerful probe of density wave and superconducting ground states. Proton NMR has been used extensively in studies of organic materials, but the protons are generally in positions far from the molecular orbitals which drive the ground state behavior. To gain access to nuclei situated more closely to the region of interest, and to study the influence of high magnetic fields on various ground states, we have undertaken the development of techniques to carry out NMR measurements in very high magnetic fields ($B > 15$ T). The initial focus of our attention has been on ^{77}Se NMR in $(TMTSF)_2PF_6$. Earlier NMR studies of powdered samples[5–7] indicate that Se is more strongly coupled to the conduction electrons than C and H nuclei, and this is supported by band structure calculations[8] which show that the Se $4s$ and $4p$ orbitals contribute significantly more to the conduction bands than other atomic orbitals. Furthermore, unlike the protons which reside in methyl groups at the ends of the TMTSF molecule, ^{77}Se has no rotational behavior which greatly simplifies the analysis of its relaxation rates. However, its natural abundance ($\approx 8\%$) and small coupling

constant ($\approx$8 MHz/T) conspire to make it a difficult nucleus to study. Nevertheless, by making use of high magnetic fields, we have succeeded in conducting ^{77}Se NMR on a single crystal of $(TMTSF)_2PF_6$.[9] The advantages of being able to study single crystals of such an anisotropic system are obvious, but we note also that the weak-coupling constant of ^{77}Se results in lower observation frequencies than for, say, ^{1}H. This not only opens the door to the possibility of separating the field and frequency dependence of NMR signals, but it also presents considerably less technical difficulties since one is able to work at sub-GHz frequencies at high fields, even in the 45 T hybrid magnet now being built at NHMFL.

The rest of this paper is organized as follows. In the next section we discuss the physical details of the title material and briefly review previous NMR measurements in this system. Section III describes our high field experimental methods. In Sec. III we report our ^{77}Se NMR results. In Sec. IV, we report our findings in regards to the metallic, partially gapped, and (our proposed) fully gapped states, and we discuss them in the context of the present understanding of metallic and SDW NMR relaxation mechanisms. In Sec. V, we present our conclusions and discuss the prospects of future high field NMR studies.

II. $(TMTSF)_2PF_6$

A. Material properties

$(TMTSF)_2PF6$ is a highly anisotropic, linear-chain conductor. Parallel chains of the TMTSF molecules form planes separated by the PF_6 complex. The anisotropy of the triclinic crystal structure (symmetry $P\bar{1}$) and the orbital overlaps gives rise to a quasi-one-dimensional (1D) Fermi surface—with transfer integral values of t_a (along the chains), t_b (between adjacent, coplanar chains), and t_c (between planes) approximately equal to 300, 30, and 1 meV, respectively.[10] At low temperatures, the quasi-1D Fermi surface is unstable with respect to perturbations of wave number $2k_F$ (nesting of the Fermi surface), and the system undergoes a SDW transition.

The features of the $(TMTSF)_2PF_6$ phase diagram (see Fig. 1) at ambient pressure have been mapped by means of various techniques including transport measurements,[11] NMR,[12–22] antiferromagnetic resonance,[23] dielectric studies,[24–26] calorimetric measurements,[27,24] susceptibility measurements,[28,29] and muon spin resonance[30] (μ^+SR).[31] The results can be summarized as follows. At T_{SDW}, a gap opens up in the electronic spectrum and the conduction electrons order antiferromagnetically, with the easy axis along b'.[32] The SDW amplitude—which is proportional to the gap—has the overall temperature dependence of the BCS gap of conventional superconductors, but recent measurements of the SDW amplitude suggest that the transition may be weakly discontinuous (first order).[19,17] Moreover, the SDW nesting is imperfect, leaving pockets of carriers in the SDW state.

B. Transport and thermodynamic studies

There is considerable experimental evidence that the SDW in $(TMTSF)_2PF_6$ is incomplete. Quantum oscillations

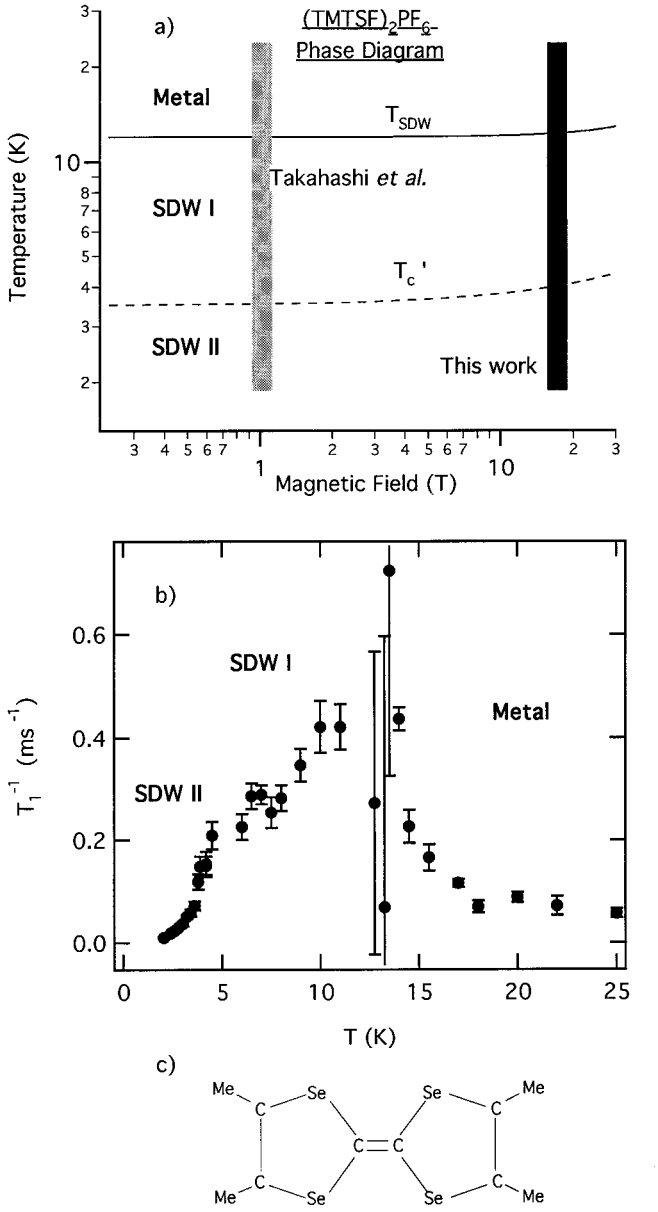

FIG. 1. (a) A schematic of the phase diagram of $(TMTSF)_2PF_6$ based on Takahashi *et al.* (Ref. 16) Uji *et al.* (Ref. 33), and this work. The proposed transition from SDW II to SDW III at $T_c'' \approx 1.5$ K is not shown. (b) The temperature dependence of T_1^{-1} over the whole range covered by the experiments ($\mathbf{H} \| \mathbf{c}^*$ axis). The error bars represent the error of the fit of a single exponential to the recovery of the magnetization (see text). (c) The TMTSF molecule. ''Me'' denotes a methyl group.

are observed in transport data below T_{SDW}. Their period corresponds to a few percent of the Brillouin Zone (BZ), but their temperature dependence departs from the standard Lifshitz-Kosevitch formalism below $\approx$4 K.[33,34] When a magnetic field is applied parallel to the least conducting axis, T_{SDW} has a quadratic field dependence up to 30 T.[33,35,36] Bjelis and Maki[37] have shown that T_{SDW} of an imperfectly nested SDW should, at low fields, increase quadratically when a magnetic field is applied along the least conducting axis of a SDW system. [At sufficiently high fields, the field dependence of T_{SDW} should saturate and in

$(TMTSF)_2NO_3$, T_{SDW} is quadratic in H up to ≈ 10 T and approaches saturation at ≈ 30 T.[1]] Furthermore, the temperature dependence of the specific heat does not change substantially upon cooling through T_{SDW}, although a weak enhancement is observed around T_{SDW}.[27]

C. Previous NMR studies

By means of ^1H NMR linewidth studies, Takahashi *et al.* have measured the SDW amplitude and its temperature dependence; from the angular dependence of the line shape, they deduce the components of the SDW nesting vector **Q** and find it to be nearly commensurate to the lattice period with components (0.5, 0.24, -0.06) along the reciprocal lattice vectors **a***, **b***, and **c***.[14] In a series of other papers,[38,39,16] they have presented ^1H relaxation rate measurements below T_{SDW} as a function of angle, pressure, and temperature. They find qualitative changes in the temperature dependence of the spin-lattice relaxation rate below T_{SDW}: at 3.5 K, the temperature dependence changes from being approximately linear in temperature to activated behavior ($\Delta \approx 11$ K) and a ''kink'' is observed in the relaxation rate T_1^{-1}, although not of such an obvious singular nature as at T_{SDW}. A similar ''kink'' is observed at roughly 1.5 K. No changes in the proton linewidth are observed concomitant to the changes in the T_1. Their results have led them to propose a phase diagram[16] with additional transitions T_c' and T_c'' which, at ambient pressure, fall approximately at 3.5 and 1.5 K, respectively (Fig. 1). With decreasing temperature, they propose that $(TMTSF)_2PF_6$ enters SDW I at T_{SDW}, SDW II at T_c', and SDW III at T_c''. Upon pressurization, these transition temperatures are observed to decrease.[16] The activation energy is insensitive to pressure.

Clark *et al.* have also carried out extensive ^1H NMR studies of the SDW state in $(TMTSF)_2PF_6$.[17–20] They also observe an enhancement in T_1^{-1} below T_{SDW} and a ''kink'' at roughly 3.5 K (albeit a considerably broader ''kink'' than that observed by Takahashi *et al.*), followed by a decrease in T_1^{-1} that can either be described as activated (with $\Delta \approx 9$ K) or fitted to T^5.[18] They, however, interpret this behavior as a frequency-dependent dynamic effect which they support by the frequency dependence of the transition temperature. Furthermore, they attribute the fast relaxation rate immediately below T_{SDW} to the phase excitations of the SDW (see Sec. IV C) and suggest that the ''kink'' occurs when $\omega_L \tau = 1$, where ω_L is the Larmor frequency and τ the fluctuation timescale of the phase excitations.[17]

Barthel *et al.* have measured the ^{13}C T_1 in $(TMTSF)_2PF_6$, and find it to be temperature independent down to roughly 4 K. Their work does not extend to lower temperatures. The relaxation rate they measured showed no particular enhancement below T_{SDW}. They attribute their results to phason relaxation.

Azevedo *et al.*[5–7] have measured the linewidth and relaxation rates of ^1H, ^{77}Se, and ^{13}C in powder samples of $(TMTSF)_2PF_6$. Their work focused on observing the change to the SDW state with pressure. At low pressures, they found a large drop in the amplitude of the ^{77}Se line compared to the metallic, high-pressure state, which they interpreted as the effect of the SDW-induced line-broadening. In ^{13}C, they found no such effect. Moreover, in their measurement of the (pressurized) metallic state Knight shift they found that the Knight shift for ^{77}Se was considerably greater than that of ^{13}C.

The nesting conditions of a (perfect) SDW are insensitive to magnetic fields and, consequently, the SDW ground state is not affected by magnetic fields,[40] except in the case of imperfect nesting as mentioned in the Introduction. As with an antiferromagnet, however, it may undergo a spin-flop transition. In a magnetic field, the orientation of the antiferromagnetic moment may flop from the easy axis to the intermediate axis.

The field at a nucleus in bulk matter is the sum of the internal fields at its site and the external field applied to the sample. The field generated by a SDW is related to the spin density

$$\boldsymbol{\rho}_{SDW} = \boldsymbol{\rho}_0 \cos(\mathbf{Q}\cdot\mathbf{r} + \phi). \tag{1}$$

Here, $\boldsymbol{\rho}_0$ denotes the temperature and field-dependent SDW moment, **Q** is the SDW nesting vector, and ϕ is the phase of the SDW. In $(TMTSF)_2PF_6$, the easy axis coincides with the b' axis, and for $\mathbf{H}\cdot\hat{b}' < H_{sf}$, where H_{sf} is the spin-flop field [0.45 T in $(TMTSF)_2PF_6$], the SDW moment will be directed along $\hat{b}'$. Above the spin-flop, the SDW flops to the intermediate axis, the a axis. For $H = 17$ T, the field would have to be oriented to within $\pm 1.5°$ of **c*** to prevent spin flop. Comparing our data to that of Takahashi *et al.*,[15] and taking into account that, at best, we were able to orient the sample to within $\pm 5°$, we conclude that the spin-flop field was exceeded in our experiment, and the antiferromagnetic moment was along the a axis.

III. NMR IN HIGH MAGNETIC FIELDS

All results presented in this paper were taken in a high homogeneity 24-T Bitter magnet (5 ppm over 3 mm) in a ^4He cryostat. An *in situ* tunable probe was built using modified commercially available tunable capacitors. The NMR coils were wound with No. 22 and No. 24 gauge copper wire. The sample used in these experiments was a single crystal weighing 8.2 mg and of dimensions $\approx 6 \times 0.8 \times 0.4$ mm^3. This corresponds to roughly 3×10^{18} spins of ^{77}Se. The sample was placed in a thin-walled glass filled epoxy (G10) holder and the holder installed in the coil. The sample orientation was adjusted manually with the estimated accuracy of $\pm 5°$. Typically, the probe was tuned to the desired frequency (with Q values in the range from 50 to a 100), and the magnet current adjusted accordingly. A Magtec commercial spectrometer was used in carrying out the experiments. All measurements made use of phase coherent pulse techniques. The magnet was calibrated to 100 ppm using a ^7Li NMR probe. The magnet current resolution was limited to 20 A which corresponds to 140 G (or, for ^{77}Se, 111 kHz).

The NMR probe was placed in a single walled stainless insert in the cryostat. The narrow geometry of the magnet required that the NMR circuit components be put in close proximity with each other, and an atmosphere of exchange gas was required to prevent arcing between the circuit components. This presented some difficulties with temperature control above 2.1 K (the superfluid transition). In strong field

gradients, diamagnetic forces act on ^{4}He gas bubbles and liquid in such a way as to expel the liquid from the center of narrow-tailed cyrostats.[41] For the field profile of the 24 T magnet used, the bubble effect occurred at fields in excess of $\approx$17 T with consequent loss of temperature control. This led us to choose to work mostly at 17 T.

Because of arcing, the power delivered to the coil was limited to 10 to 30 W. $H_1 \propto \sqrt{P}$, where P is the power transmitted to the probe, and the $\pi/2$ pulses were of the order of 5 to 15 μs which spans the spectral width of 200 to 80 kHz, a considerably narrower width than that of the absorption line inside the SDW state. Since we were unable generate pulses short enough (high enough voltage) to cover the spectral width of the absorption line below T_{SDW}, we measured the SDW absorption line widths by compiling a histogram of the absorption amplitude as a function of field at a fixed frequency, much as in a CW measurement.

In T_1 measurements, a comb of $\pi/2$ pulses was used for saturation. The recovery of the magnetization was then followed over at least one decade using $\pi/2-\pi$ pulses. In T_2 measurements, $\pi/2-\pi/2$ and $\pi/2-\pi$ pulse sequences were used, and the decay of the magnetization was then followed over at least one decade. The error bars on the T_1 and T_2 data presented in the following sections reflect the error of a single exponential fit to the time evolution of the recovery or decay of the nuclear magnetization and, except at temperatures close to T_{SDW}, most are of that order. In our relaxation rate measurement we estimate the maximum attainable accuracy to be around 10% in T_1 which is similar to what has been achieved previously.[21]

The availability of power poses constraints on the use of resistive magnets for NMR and our results were gathered over a six month period. To ensure consistency, T_1 was measured at 4.2 K on each occasion and found to differ only to within a few percent for a given orientation.

IV. RESULTS

The temperature dependence of T_1^{-1} at 17 T over the complete range of our investigation is shown in Fig. 1. Three distinct regions of T_1^{-1} behavior are seen which correspond to the metallic state ($T_{\mathrm{SDW}}<T$), the first SDW state ($T_c'<T<T_{\mathrm{SDW}}$), and the onset of activated behavior ($T<T_c'$). In the following sections we describe in turn these three regimes and also examine the behavior of key features in the resonance spectrum at the transition temperatures T_{SDW} and T_c'.

A. Metallic state

A detail of the behavior of T_1^{-1} in the metallic state between 30 and T_{SDW} ($\approx$13 K at 17 T) is shown in (Fig. 2). Our results are consistent with the notion of Korringa-like relaxation in the metallic state, with deviations as T_{SDW} is approached. This interpretation is, however, complicated by the fact that the charge transport along the least conducting axis degrades at high temperatures and a change occurs in the effective dimensionality of the transport. Earlier measurements by Wzietek *et al.*[21] have shown that at $T\approx$100 K, the relaxation departs from the Korringa law. At the upper end of the temperature range we studied, we assume that the

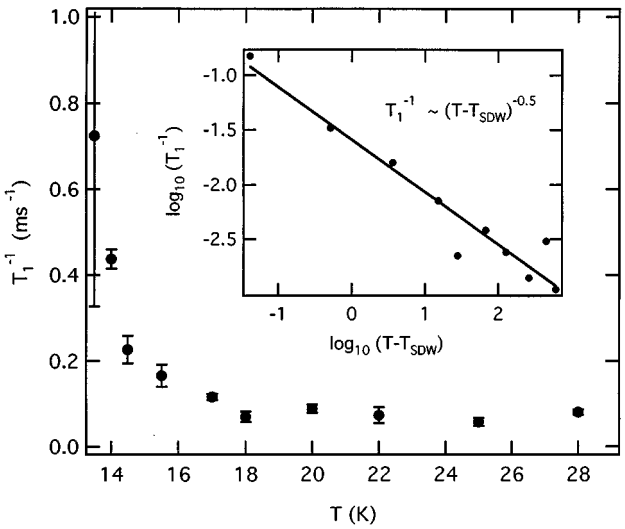

FIG. 2. T_1^{-1} vs T above T_{SDW}. The inset shows $\ln(T_1^{-1})$ vs $\ln(T-T_{\mathrm{SDW}})$.

fluctuations associated with the SDW transition are weak and that the temperature dependence of T_1^{-1} is crossing over to $T_1^{-1}\propto T$, but the range and resolution of our data do not allow us to determine this unambiguously.

The scaling of T_1^{-1} exhibited in the inset is consistent with that of a 3D antiferromagnetic transition[42] first reported by Wzietek *et al.*[21]: $T_1^{-1} \sim (T-T_{\mathrm{SDW}})^{-\nu}$, $\nu=0.48\pm0.05$ [where ν is obtained by a linear fit of $\ln(T_1^{-1})$ vs $\ln(T-T_{\mathrm{SDW}})$; the error quoted is the error of the fit]. This suggests that fluctuations are important over temperature scales on the order of at least 1 K around T_{SDW}. We contrast this with calorimetric data[27] where the signature of the incipient transition starts at 0.3 K above T_{SDW}.

In addition, we have measured the temperature dependence of T_2^* and the Knight shift over the same temperature range, as shown in Fig. 3. (The fourth inequivalent ^{77}Se site is unresolved for $H\|\mathbf{c}^*$, probably because of the tilt away from the axis of rotational symmetry c). We may fit the three observed absorption lines to a composite Lorentzian over the whole temperature range, as also shown in Fig. 3, and thereby obtain the temperature dependence of the line shift (i.e., the Knight shift) and T_2^*. The latter we estimate by the full width at half maximum (FWHM) of each line: $(2/T_2^*)^{-1}=$FWHM (Fig. 3). We find the Knight shift to be temperature independent, reflecting the metallic nature of $(\mathrm{TMTSF})_2\mathrm{PF}_6$ in the temperature range immediately above T_{SDW}. T_2^*, however, is observed to decrease upon approaching the transition. Qualitatively, it is to be expected that the spin-spin relaxation rate increases when the critical fluctuations preceding the phase transition slow down upon approaching T_{SDW}.

The data above T_{SDW} in the metallic phase shows different temperature dependences for T_1^{-1} and the Knight shift. T_1^{-1} depends on the summation of $\chi(q)$ over all q vectors, with $\chi(2k_F,T)$ the dominant one for a 1D conductor. In contrast, the Knight shift depends only on the static term $\chi(q=0)$. This difference in temperature dependence most likely arises since $\chi(q=0)$ has a different temperature de-

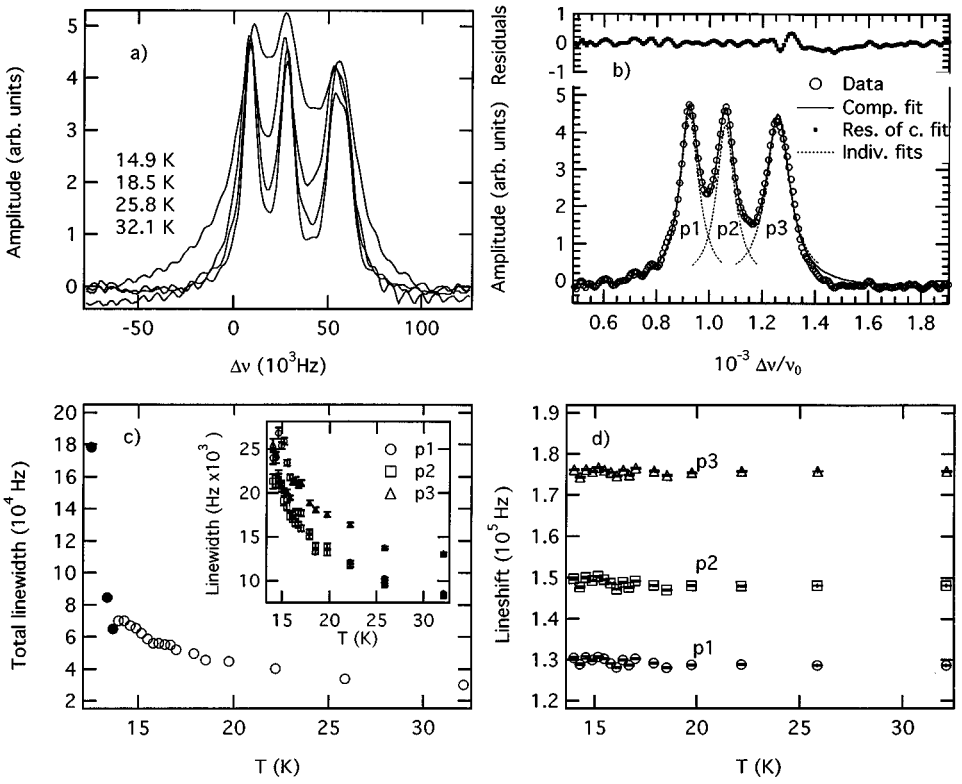

FIG. 3. (a) Fourier transformed spin echoes (from top to bottom: at 14.9, 18.5, 25.8, and 32.1 K) at several different temperatures in the metallic phase. (b) A Fourier transformed spin echo and the corresponding numerically fitted Lorentzian absorption lines. $H\|\mathbf{c}^*$ axis, $H=17$ T, $T=17$ K. The shift is with respect to $\nu_0=\gamma|\mathbf{H}|/2\pi$. (c) The linewidth and the (d) line shift in the metallic state as obtained by a Lorentzian fit to the absorption spectrum. (c) plots the sum of the FWHM $(2/T_2^*)$ of the three absorption lines depicted in (b). This gives a measure of the total linewidth. The solid markers show the FWHM of the SDW absorption spectrum as fitted by a single Lorentzian. The insert to (c) shows the FWHM of the individual lines $p1$, $p2$, and $p3$ labeling the peaks in (b) from left to right. (d) The line shifts of the three absorption peaks with respect to $\nu_0=\gamma|\mathbf{H}|/2\pi$.

pendence than $\Sigma\chi(q,\omega)$, where the latter contains weakly divergent behavior near T_{SDW}.

B. The SDW state

Our T_1 data below T_{SDW} is shown in Fig. 4. Between T_{SDW} and T_c' the temperature dependence of T_1 is strikingly Korringa-like. Qualitatively, it resembles that of Takahashi *et al.*: as in Ref. 16, the temperature dependence of T_1^{-1} is at first approximately linear, and then T_1^{-1} decreases precipitously below T_c'. The only notable difference between our ^{77}Se and Takahashi's proton data is that in our case, the ''kink'' at T_c' more resembles a ''shoulder'' and it occurs at a higher temperature, 4.0 ± 0.2 K. Although we have not yet systematically investigated T_c' as a function of magnetic field, and therefore frequency, it may be that T_c' is field and/or frequency dependent. Since T_{SDW} increases with field, a similar behavior of T_c' is certainly likely. Indeed, Musfeldt *et al.*[43] have observed a shift upwards in temperature in T_c' at lower fields (up to 3 T) in measurements of the dynamic dielectric constant where frequencies two orders of magnitude greater than the ^{77}Se NMR frequency were used (16 GHz vs 136 MHz).

We further note that T_1 becomes activated below T_c' (Fig. 5) with the activation energy apparently changing from 12.7 to 8.0 K at ≈ 3 K which agrees reasonably with the values of $\Delta=11$ K and $\Delta=9.2$ K previously reported.[16,18] The gap value(s) is also in good agreement with that obtained from transport.[33] We note also that T_1^{-1} vs T is well approximated by T^5, in agreement with earlier NMR results.[18] The data clearly suggests that there are two distinct relaxation mechanisms at work above and below T_c'.

The temperature variation of the composite SDW linewidth measurements is shown in Fig. 6. Both the line shift and the linewidth are seen to be temperature independent, to within error, over the range shown. The fractional lineshift ν/ν_0, is $\approx 4.2\times10^{-4}$, about 10 times less than in the metallic phase. Qualitatively, this is consistent with the suppression of the metallic state Pauli susceptibility in the SDW phase. The linewidth is consistent with a static internal field of approximately 350 G. We note that neither the linewidth nor the line shift change significantly upon cooling below T_c' which puts constraints upon the nature of the transition. Both are probably dominated by the SDW wave in the SDW I phase, so the change, if any, to the structure of the SDW in going from SDW I to II must be small.

C. Relaxation in SDW I

In Fig. 4 we plot $(T_1T)^{-1}$ vs T below T_{SDW}. It is essentially constant between T_{SDW} and T_c' as one would expect for Korringa relaxation. This relaxation behavior is consistent with the existence of free carriers, electrons, or holes in an

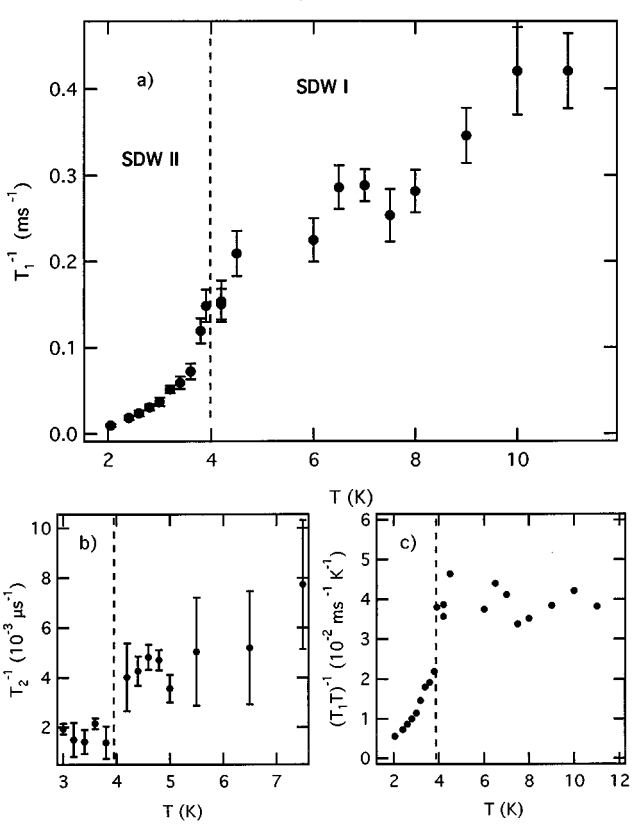

FIG. 4. (a) T_1^{-1} vs T below T_{SDW}. (b) T_2^{-1} vs T in the SDW phase. (c) $(T_1T)^{-1}$ vs T.

incompletely nested SDW. If this is the case, the enhancement of T_1^{-1} below T_{SDW} is caused by the Fermi level's cutting across the bottom (or top) of an electron (or hole) band where the density of states is greater than at the Fermi level in the metallic state.

The SDW, however, has three possible types of excitations which could also provide a relaxation mechanism in SDW I. They are antiferromagnetic magnons and excitations which correspond to fluctuations in the phase and amplitude, respectively. The amplitude fluctuations have characteristic energies larger than the SDW gap[2] and can be ruled out. Hanson has argued that the magnon contribution to ^{1}H spin-lattice relaxation in the SDW state is small.[17] This leaves the phase fluctuations, or phasons. Their dispersion relation (for $q \ll 2k_F$) is $\omega_\phi(q) = v_F q$ where the Fermi velocity v_F is taken to be that of the metallic state since a SDW transition does not change the band mass.[2]

We therefore consider the recent prediction for the SDW phason relaxation rate proposed by Clark *et al.*[20] [Eq. (2)]. In a simple model connecting the fluctuating fields at a nucleus to the phasons, they predict that

$$\frac{1}{T_1} = \frac{\gamma_2 k_B T \langle \delta H_\perp^2 \rangle \alpha''(\omega)}{2\lambda^2 \omega \epsilon^2}, \tag{2}$$

where $\langle \delta H_\perp^2 \rangle$ is the mean squared amplitude of fluctuating field perpendicular to the static external field, λ is the SDW wavelength, ω is the NMR observation frequency, and $\alpha''(\omega)$ is the imaginary part of the polarizability. $\alpha''(\omega)$ is related to the complex dielectric constant via

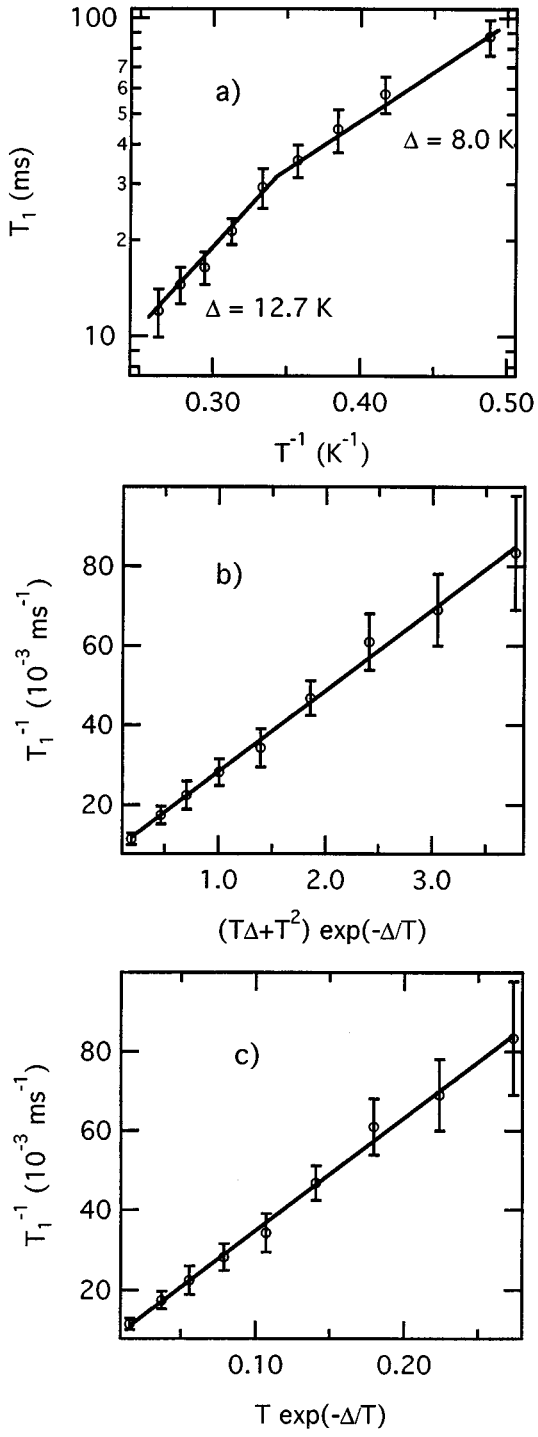

FIG. 5. (a) $\ln(T_1^{-1})$ vs T^{-1} in the SDW state below 4 K. The average gap value over the whole temperature range is $\Delta = 10.0 \pm 0.5$ K. (b) T_1^{-1} vs $(T\Delta + T^2)e^{-\Delta/kT}$. (c) T_1^{-1} vs $Te^{-\Delta/kT}$.

$\epsilon = 1 + 4\pi N\alpha$, $\epsilon'' = 4\pi N\alpha''$ (N being the volume density of the SDW waves).[44] If ω and $\langle \delta H_\perp \rangle$ are constant, this relation has the same temperature dependence as the Korringa mechanism, but it has the advantage that we can use it to estimate T_1 or, having measured T_1, estimate ϵ''. Using the value of the fluctuating field obtained by assuming $\omega\tau = 1$ (see Sec. IV D), we calculate the magnitude of ϵ'' at 136 MHz and 4.2 K. It is approximately an order of magnitude

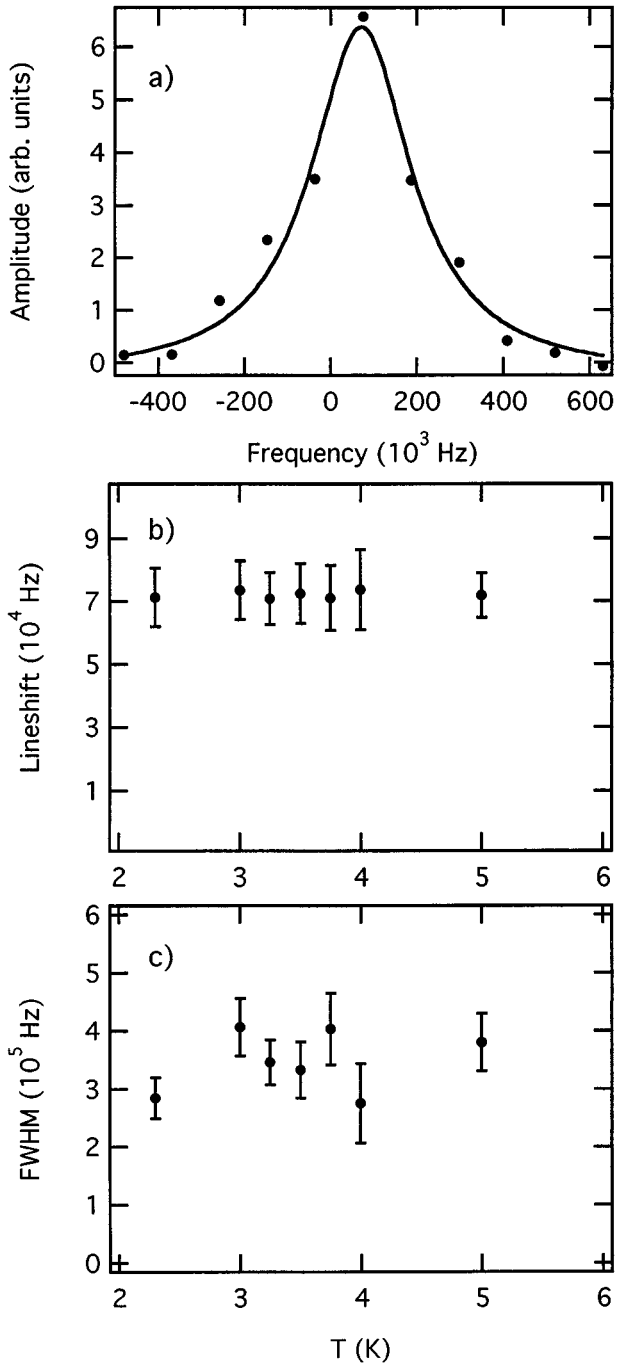

FIG. 6. (a) A composite SDW linewidth at 20.4 T and $\mathbf{H}\|\mathbf{c}^*$. (b) the line shift with respect to $\gamma/2\pi H$ as a function of temperature. (c) the linewidth as a function of temperature.

smaller than ϵ'' measured by Nad *et al.* at 10 MHz and 4 K.[25] Their measurements of ϵ'' extend only to 10 MHz and, at 4 K, show it to decrease monotonically with higher frequencies, consistent with simple Drude-like behavior. While the agreement is strikingly good, the uncertainty in our estimate of $\langle \delta H^2 \rangle$ and the lack of a direct measurement of ϵ'' in the 100 MHz make this quantitative comparison inconclusive.

To summarize, we cannot distinguish between the metallic and SDW relaxation mechanisms because they both have the same temperature dependence. A detailed investigation of the frequency dependence of T_1 in the SDW phase is needed to determine which relaxation mechanism dominates between T_{SDW} and T_c'.

D. Relaxation below T_c'

We next address the nature of the relaxation mechanism below T_c'. In essence, we propose that the SDW I relaxation is provided by the residual carriers at the Fermi level, and the SDW gap becomes complete below T_c', extinguishing the Korringa relaxation. Our argument is based on the consideration of the spin-lattice relaxation rate of the itinerant spins in a semiconductor.[45] Here the Boltzman distribution is substituted for the Fermi distribution before performing the integration over energy, weighed by the density of states, that sums the relaxation contributions of the itinerant carriers. In the case of a metal, it is the integration over the probability of occupation and vacancy of the initial and final states of the electrons, respectively, weighed by the density of states at the initial and final energy levels E_i and E_f that gives the Korringa relaxation rate T_1^{-1}. Specifically, the integration is over the expression

$$\rho(E_i)\rho(E_f)f(E_i)[1-f(E_f)]|\langle i|\mathcal{H}|f\rangle|^2\delta(E_i-E_f+\gamma_n H) \tag{3}$$

(where the last two factors describe the electron-nuclear interaction). In the case of the Fermi function $f(E_i)[1-f(E_f)]\approx kT\delta(E_i-E_f)$ and $E_i\approx E_f\approx E_F$, and the $T_1^{-1}\propto T\rho^2(E_F)$ relation emerges. We draw attention to the fact that this expression is independent of dimensionality as expressed in the dimensional effects on the functional dependence of the density of states on energy. Because of the term $\delta(E_i-E_f)$, the functional dependence of the density of states on energy does not affect the integration.[46]

Consider now substituting the Boltzmann distribution $P(E)=ae^{-E/kT}$ for the Fermi distribution. We assume that $kT\ll\Delta$ for the Fermi distribution, which seems justifiable based on how well the data is fitted by this approximation. In the case of a sparsely filled band,[45] a is obtained by the constraint that an integration over $\rho(E)P(E)$ from the bottom of the band, arbitrarily chosen as 0, to infinity, should yield the total (and constant) number of carriers n. In our case, the number of carriers is temperature dependent, and a can be taken as unity. Omitting the electron-nuclear interaction terms and bearing in mind that $E_i\approx E_f$, one finds that

$$\frac{1}{T_1}\propto\int_\Delta^\infty \rho^2(E)e^{-E/kT}dE, \tag{4}$$

where Δ is the gap energy. Here, the dimensionality of the system comes into play via $\rho(E)$ which is proportional to $E^{1/2}$ in 3D but constant in 2D. (We do not consider strict 1D calculations to be appropriate in this system). In each case, this leads to relaxation rates proportional to $(T\Delta+T^2)e^{-\Delta/kT}$ and $Te^{-\Delta/kT}$, respectively.

This approach is motivated by the fact that below T_c', T_1 does not appear to be strictly activated, but by including the effect of the density of states, as in the calculation above, we predict relaxation rates which are in excellent agreement with the data. Unfortunately, the predicted behaviors of a 2D

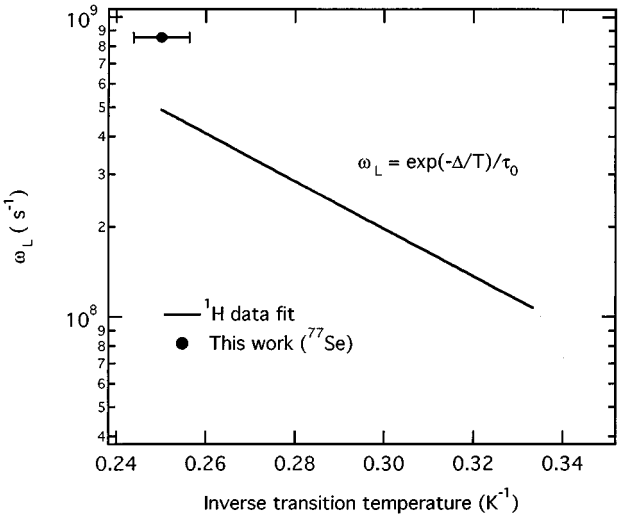

FIG. 7. A comparison of the ^{77}Se transition temperature at 136 MHz ($H=17$ T), with the frequency dependent ^{1}H transition temperature as measured by Hanson (Ref. 17).

and a 3D system are indistinguishable for a gap of $\Delta \approx 10$ K in the temperature range we covered.

We have also measured T_2^{-1} in the SDW state. We find that it decreases by a factor of 3, from roughly 0.2 to 0.6 ms upon cooling below T_c'. The T_2^{-1} data is shown in Fig. 4. The noise of the data prevents one from making any definitive statements about the nature of the temperature dependence other than that T_2^{-1} decreases at T_c'. However, T_1^{-1} and T_2^{-1} are connected by[47]

$$\frac{1}{T_1}=\frac{\gamma^2\tau_0}{1+\omega_0^2\tau_0^2}(h_x^2+h_y^2), \quad \frac{1}{T_2}=\frac{1}{2T_1}+\gamma^2 h_z^2\tau_0, \quad (5)$$

where h_i is the $i=x,y,z$ component of the fluctuating field (z being the direction of H), τ_0 is the fluctuating time scale, and ω_0 is the angular frequency of the NMR resonance. It could be that the decrease in T_2^{-1} is attributable to the vanishing contribution of the T_1^{-1} term in Eq. (5). This would leave a residual $T_2^{-1}\approx\gamma^2 h_z^2\tau_0$. In the limit of fast fluctuations, $\tau_0 \ll T_1$, T_2, and the convergence of T_1 and T_2 can then be explained as arising from a change in the anisotropy of the fluctuating field. When $h_x=h_y=h_z$ [Eq. (5)], $T_1=T_2$.

The slower relaxation rates below T_c' can also possibly be attributable to the decrease in the spectral density of the fluctuations at the Larmor frequency ω_L.[17] When $\omega_L \approx 1/\tau_0$, a peak will appear in T_1^{-1}. The data of Clark and collaborators, unlike ours and that of Takahashi and collaborators, exhibit a weak peak in T_1^{-1} at T_c'. If such a peak is brought about by the coincidence of ω_L and τ_0^{-1}, T_c' should appear activated when plotted as a function of frequency:[47]

$$w_L=\frac{1}{\tau_L}e^{-\Delta/kT}. \quad (6)$$

Clark and co-workers[17] studied the frequency dependence of T_c' and found that it fits this law rather well with $\Delta \approx 18$ K. We plot their data and our location of T_c' with respect to frequency and temperature in Fig. 7. While our peak does not fall exactly on their ω_L vs T^{-1} curve, the different qualitative temperature dependence of the T_1^{-1} data and the possibly different criteria we may use to identify the exact position of the peak in temperature (they have greater point density with respect to temperature but a considerably broader feature) may explain the discrepancy. Likewise, the weaker coupling of the protons to the SDW could explain why they observe the peak at a different frequency than we do.

Assuming that the dynamical crossover of the type proposed by Clark and co-workers is a true description of T_c', one can use Eq. (5) to estimate the perpendicular and parallel components of the fluctuating fields h_i at T_c', using the measured values of T_1 and T_2. We obtain $h_\perp \approx h_\parallel \approx 115$ G. One expects the magnitude of the fluctuating field to be considerably smaller than the total amplitude of the internal field of the SDW: if the phasons provide the dominant relaxation mechanism in the SDW state of $(TMTSF)_2PF_6$, the physical displacement of the SDW giving rise to the fluctuating field should only be a fraction of the SDW period, causing each nucleus to see, on average, a change in field corresponding to a fraction of the total SDW amplitude. The latter we estimate (from the linewidth) as ≈ 350 G, so h can be considered physically plausible.

V. CONCLUSION

We report on a very high magnetic field study of the ^{77}Se NMR spectrum and relaxation in the material $(TMTSF)_2PF_6$ which exhibits a complex ground-state behavior in the range of temperature below $T_{SDW} \approx 12$ K. In terms of the pain lattice relaxation behavior (T_1^{-1}), we observe a transition from metallic to spin fluctuation behavior which scales as a power law of $(T-T_{SDW})$ as the critical temperature is approached. Below T_{SDW}, we find that within the main SDW phase the value of T_1 is greater than in the metallic phase, but that the temperature dependence is Korringa-like. We interpret this behavior as a result of the coexistence of both conduction electrons (holes), left over because of the imperfect nesting of the Fermi surface (causing an incomplete SDW gap) and the SDW phase. We find that reasonable models for spin (phason) relaxation have the same temperature dependence as the conduction (Korringa) mechanism and cannot be separated for a constant frequency (magnetic field). We further propose that a detailed frequency (magnetic field) study can help in separating these terms. We note, however, that there may be magnetic field-dependent effects (such as on T_{SDW}) which are independent of frequency. Below a lower temperature, $T_c'(\approx 4$ K), we observe an activated behavior of T_1 in temperature. We propose that below T_c', the SDW gap becomes complete and that the Korringa relaxation mechanism is removed. A simple Boltzman activation model provides an excellent description of the results. We demonstrate that very high field NMR on a nucleus (^{77}Se) distinctly different from previous proton studies at lower fields provides a similar description of the $(TMTSF)_2PF_6$ ground state and, furthermore, opens the way to future studies of these materials in very high magnetic fields.

ACKNOWLEDGMENTS

The experiments were carried out at the National High Magnetic Field Laboratory (NHMFL) in Tallahassee, Florida. NHMFL is supported by the NSF and the State of Florida. We wish thank the staff of NHMFL for miscellaneous assistance. We acknowledge useful discussions with P. Sandhu, N. Sullivan, and S. Uji. This research is supported in part by NSF Grant No. DMR 95-10427.

[1] A. Audouard and S. Askenazy, Phys. Rev. B **52**, 700 (1995).
[2] G. Grüner, *Density Waves in Solids* (Addison-Wesley, London, 1994).
[3] T. Ishiguro and K. Yamaji, *Organic Superconductors* (Springer, New York, 1990).
[4] J. Wosnitza, *Fermi Surfaces of Low-Dimensional Organic Metals and Superconductors* (Springer, New York, 1996).
[5] L. J. Azevedo, J. E. Schirber, and J. C. Scott, Phys. Rev. Lett. **49**, 826 (1982).
[6] L. J. Azevedo, J. E. Schirber, and E. M. Engler, Phys. Rev. B **27**, 5842 (1983).
[7] L. J. Azevedo, J. E. Schirber, and E. M. Engler, Phys. Rev. B **29**, 464 (1984).
[8] T. Mori, A. Kobayashi, Y. Sasaki, and H. Kobayashi, Chem. Lett. **19**, 1923 (1982).
[9] The signal to noise ratio in a NMR experiment is proportional to $NI(I+1)\gamma^{5/2}(H/k_BT)^{3/2}$, where N is the number of spins, γ the coupling constant, H the field, I the spin quantum number of the nucleus, k_B the Boltzman factor, and T the temperature (see Ref. 45).
[10] P. Grant, J. Phys. (France) Colloq. **44**, C3-847 (1983).
[11] K. Bechgaard *et al.*, Solid State Commun. **33**, 1119 (1981).
[12] A. Andrieux, D. Jerome, and K. Bechgaard, J. Phys. (France) Lett. **42**, 187 (1981).
[13] J. C. Scott *et al.*, *Proceedings of the International Conference on Low-Dimensional Conductors, Boulder, Colorado* (Gordon and Breach, New York, 1982).
[14] T. Takahashi, Y. Maniwa, H. Kawamura, and G. Saito, J. Phys. Soc. Jpn. **55**, 1364 (1986).
[15] T. Takahashi, Y. Maniwa, H. Kawamura, and G. Saito, Physica B **143**, 417 (1986).
[16] T. Takahashi *et al.*, Synth. Met. **41**, 3985 (1991).
[17] M. E. Hanson, Ph.D. thesis, UCLA, 1994.
[18] W. H. Wong *et al.*, Phys. Rev. Lett. **70**, 1882 (1993).
[19] W. G. Clark, M. E. Hanson, W. H. Wong, and B. Alavi, Physica B **285**, 194 (1994).
[20] W. G. Clark *et al.* (unpublished).
[21] P. Wzietek *et al.*, J. Phys. (France) I **3**, 171 (1993).
[22] E. Barthel *et al.*, Europhys. Lett. **21**, 87 (1993).
[23] J. B. Torrance, H. J. Pedersen, and K. Bechgaard, Phys. Rev. Lett. **49**, 880 (1982).
[24] J. C. Lasjaunias *et al.*, Phys. Rev. Lett. **72**, 1283 (1994).
[25] F. Nad, P. Monceau, and K. Bechgaard, Solid State Commun. **95**, 655 (1995).
[26] J. L. Musfeldt, M. Poirer, P. Batail, and C. Lenoir, Phys. Rev. B **51**, 8347 (1995).
[27] J. Coroneus, B. Alavi, and S. E. Brown, Phys. Rev. Lett. **70**, 2332 (1993).
[28] K. Mortensen, Y. Tomkiewicz, T. D. Schultz, and E. M. Engler, Phys. Rev. Lett. **46**, 1234 (1981).
[29] K. Mortensen, Y. Tomkiewicz, and K. Bechgaard, Phys. Rev. B **25**, 3319 (1982).
[30] L. P. Le *et al.*, Europhys. Lett. **15**, 547 (1991).
[31] For an overview, we refer the reader to Refs. 3,2,4.
[32] a, b, and c are nonorthogonal and $\mathbf{a}^*$, $\mathbf{b}^*$, and $\mathbf{c}^*$ denote the reciprocal lattice vectors orthogonal to the b and c, a and c, and the a and b axes, respectively. b' and c' are the projections of b and c on to the plane perpendicular to the a axis.
[33] S. Uji, Phys. Rev. B **55**, 12 446 (1997).
[34] J. P. Ulmet *et al.*, J. Phys. (France) Lett. **46**, 535 (1985).
[35] G. M. Danner, P. M. Chaikin, and S. T. Hannahs, Phys. Rev. B **53**, 2727 (1996).
[36] N. Biskup, S. Tomic, and D. Jerome, Phys. Rev. B **51**, 17 972 (1995).
[37] A. Bjelis and K. Maki, Phys. Rev. B **45**, 12 887 (1992).
[38] H. Kawamura *et al.*, Jpn. J. Appl. Phys. Suppl. **26-3**, 583 (1987).
[39] T. Takahashi *et al.*, Synth. Met. **19**, 225 (1987).
[40] L. P. Gor'kov and A. G. Lebed, J. Phys. (France) Lett. **45**, L433 (1984).
[41] E. J. McNiff, Jr. *et al.*, Rev. Sci. Instrum. **59**, 11 (1988).
[42] C. Bourbonnais, J. Phys. (France) I **3**, 143 (1993).
[43] J. L. Musfeldt, M. Poirer, P. Batail, and C. Lenoir, Phys. Rev. B **52**, 15 893 (1995).
[44] The expression shown here is our rederivation of Clark's expression and, apart from a factor of $4\pi N/\hbar$, it is identical to his.
[45] A. Abraham, *Principles of Nuclear Magnetism* (Oxford, New York, 1961).
[46] We ignore certain complications such as the effect of Landau level quantization in 2D. Such dimensional effects on NMR relaxation rates in 2D systems have been discussed by Vagner and Maniv, Physica B **204**, 141 (1995).
[47] C. P. Slichter, *Principles of Magnetic Resonance* (Springer, New York, 1990).